A baseband LPF for GSM, TD-SCDMA and WCDMA multi-mode transmitters*

Yu Yongchang(余永长), Han Kefeng(韩科锋), Wang Lifang(王丽芳), Tan Xi(谈熙)†, and Min Hao(闵昊)

State Key Laboratory of ASIC & System, Fudan University, Shanghai 201203, China

Abstract: This paper describes a low-pass reconfigurable baseband filter for GSM, TD-SCDMA and WCDMA multi-mode transmitters. To comply with 3GPP emission mask and limit TX leakage at the RX band, the out-of-band noise performance is optimized. Due to the distortion caused by the subthreshold leakage current of the switches used in capacitor array, a capacitor bypass technique is proposed to improve the filter's linearity. An automatic frequency tuning circuit is adopted to compensate the cut-off frequency variation. Simulation results show that the filter achieves an in-band input-referred third-order intercept point (IIP3) of 47 dBm at 1.2-V power supply and the out-of-band noise can meet TX SAW-less requirement for WCDMA & TD-SCDMA. The baseband filter incorporates –40 to 0 dB programmable gain control that is accurately variable in 0.5 dB steps. The filter's cut-off frequency can be reconfigured for GSM/TD-SCDMA/WCDMA multi-mode transmitter. The implemented baseband filter draws 3.6 mA from a 1.2-V supply in a 0.13 μm CMOS process.

Key words: active-RC filter; multi-mode transmitter; analog baseband; tuning circuit
DOI: 10.1088/1674-4926/32/2/025003 **EEACC:** 1270

1. Introduction

With the booming of wireless communications, multi-mode cellular radios have been driving single chip integration and SAW-less for lower cost and a smaller area. A reconfigurable baseband filter shown in Fig.1 serves as a reconstruction filter for the D/A converter in the multi-mode transmitter. It is used to reject out-of-band noise emissions and provide gain control for the transmitter. The required stopband attenuation is derived from the spurious emission mask. The transfer function is based on a fourth-order Chebyshev low pass filter prototype with 0.1 dB in-band ripple. The active-RC Tow-Thomas biquad is selected due to its low sensitivity to PVT variation, good linearity performance and gain accuracy. To comply with the 3GPP spurious emission mask, the out-of-band noise performance of the baseband filter is optimized. The last operational amplifier shown in Fig. 1 and R_{a2} contributes the main out-of-band noise. So a low noise operational amplifier is used for the last one in the cascade biquads. Due to the high leakage current in deep-submicrometer process, the linearity of the filter with switched capacitor array is deteriorated. The CB technique is proposed to improve the baseband filter's linearity performance. To minimize the near-far effect, mobile transmitters have to provide large gain control range, i.e., 74 dB for WCDMA, 73 dB for TD-SCDMA and 30 dB for DCS. As shown in Fig. 1, the programmable gain control is realized by switchable resistors and the gain variation range is from –40 to 0 dB in 0.5 dB steps. The cut-off frequency switching is realized by switchable capacitor arrays. The filter has switchable cut-off frequency from 0.3 to 3.6 MHz in 0.3 MHz steps. The flexible cut-off frequency switching facilitates minimizing EVM. Because the peak-to-peak voltage of the filter's input signal might be up to 800 mV, which is large compared to the in-band noise floor, the EVM is mainly caused by the phase distortion and magnitude distortion. The phase distortion can be reduced by setting the cut-off frequency higher than the channel bandwidth because the maximum group delay occurs nearly at the cut-off frequency (Fig. 2).

2. Out-of-band noise analysis and design

To comply with the 3GPP emissions mask, the out-of-band noise performance should be carefully characterized. When transmitting in WCDMA band (1920 to 1980 MHz), the nearest frequency offset to the DCS band (1805 to 1880 MHz) is 40 MHz. The spurious emission requirement is restricted to be lower than –71 dBm/100 kHz[1]. The maximum output power requirement is 24 dBm in power class 3. The required signal to noise ratio (S/N) is expressed as

$$S/N = 24 - \left(-71 - 10\lg 10^5\right) = 145\ \text{dBc/Hz}. \quad (1)$$

The TX noise at 40 MHz offset is expected be lower than –148 dBc/Hz (with 3 dB margin). Due to the limited TX-to-RX isolation, transmitter out-of-band noise may leak through to the receiver and desensitize the receiver's input, as shown in Fig. 3. The WCDMA TX-RX frequency separation is 190 MHz. So the out-of-band noise floor need to be lower than –158 dBc/Hz at 190 MHz offset for SAW-less TX[2]. The out-of-band noise of baseband filter can be a bit higher than this value because the modulator's filter characteristic reduces the baseband filter's out-of-band noise at 190 MHz offset.

There are three bands for TD-SCDMA, i.e. 1880–1920, 2010–2025, and 2300–2400 MHz. The nearest DCS recep-

* Project supported by the Important National Science & Technology Specific Projects (No. 2009ZX01031-003-002) and the National High Technology Research and Development Program of China (No. 2009AA011605).
† Corresponding author. Email: tanxi@fudan.edu.cn
Received 21 July 2010, revised manuscript received 31 August 2010

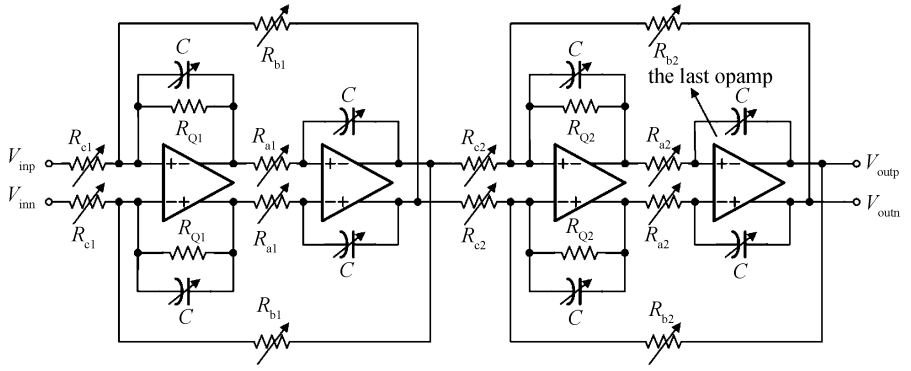

Fig. 1. Baseband low pass filter.

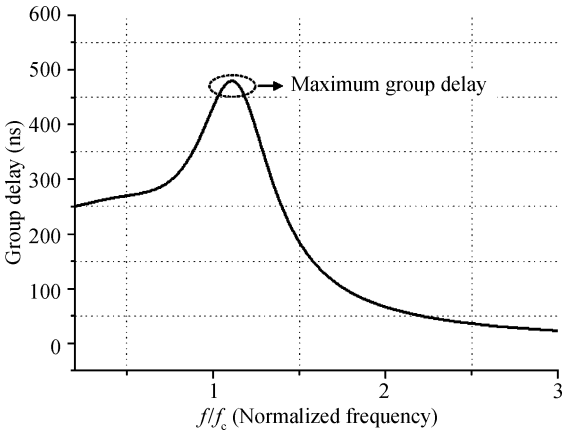

Fig. 2. Group delay.

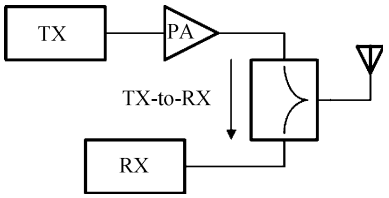

Fig. 3. Transmitter leakage into the receiver.

tion band is 1805–1850 MHz in China, which leaves a 30 MHz guard band. The spurious emission requirement is –71 dBm/100 kHz. The maximum output power requirement is 24 dBm in power class 2. The TX noise at 30 MHz offset is expected be lower than –148 dBc/Hz (with 3 dB margin). TD-SCDMA is a TDD system and there is no TX-to-RX leakage problem as mentioned above.

The most stringent spurious emission requirement is the out-of-band noise at 20 MHz offset which is defined by 3GPP and the spurious emission requirement is –79 dBm/100 kHz. The maximum output power requirement is 33 dBm. So the TX noise at 20 MHz offset is expected to be lower than –162 dBc/Hz.

The baseband filter consists of two biquads in cascade. The main noise contributors are identified as the last operational amplifier in the second biquad as well as resistor R_{a2} shown in Fig. 1. All other contributors already attenuated by the filter characteristic of the second biquad. The noise transfer function (NTF) of the operational amplifier and R_{a2} are expressed as

$$V_{o,n1} = \sqrt{2}\frac{sR_{Q2}C + 1}{s^2 R_{a2} R_{Q2} C^2 + sR_{a2}C + \dfrac{R_{Q2}}{R_{b2}}} V_{R_{a2,n}}, \quad (2)$$

$$V_{o,n2} = \frac{s^2 R_{a2} R_{Q2} C^2 + s\left(R_{Q2} + R_{a2}\right)C + 1}{s^2 R_{a2} R_{Q2} C^2 + sR_{a2}C + \dfrac{R_{Q2}}{R_{b2}}} V_{op,n}, \quad (3)$$

where $V_{o,n1}$ and $V_{o,n2}$ are output noise contributors caused by R_{a2} and the last operational amplifier respectively. The $V_{R_{a2},n}$ is the noise voltage of R_{a2} and $V_{op,n}$ is the equivalent input noise voltage of the last operational amplifier. R_{a2}, R_{b2}, R_{Q2} and C are shown in Fig. 1. According to Eqs. (2) and (3), the out-of-band noise can be reduced by decreasing R_{a2} and $V_{op,n}$. Decreasing R_{a2} makes capacitor C larger to keep RC constant and more power consumption is needed for operational amplifier to drive smaller R and larger C. The $V_{op,n}$ can be reduced by increasing the power consumption of the last operational amplifier.

3. Linearity analysis and design

To minimize interference to neighboring channels, an adjacent channel leakage ratio (ACLR) is defined by 3GPP. The ACLR is dependent on the device nonlinearity. The n-tone ACLR formula is[3]:

$$\begin{aligned}\mathrm{ACLR} = {} & 2\left(P_{2\_\mathrm{tone}} - \mathrm{OIP_3}\right) \\ & - 10\lg\frac{n^3}{2\left(\dfrac{2n^3 - 3n^2 - 2n}{3} + \varepsilon\right) + (n^2 - \varepsilon)} \\ & - 6\ \mathrm{dB},\end{aligned} \quad (4)$$

where

$$\varepsilon = \mathrm{mod}\left(\frac{n}{2}\right) = \text{the division remainder of } n \text{ by } 2. \quad (5)$$

In Eq. (4), P_{2_tone} is the total power of the two tones at the device's output and $\mathrm{OIP_3}$ is the output third-order intercept point of the nonlinearity device. When the filter has superior linearity performance, its nonlinearity contribution to the transmitter's ACLR can be negligible.

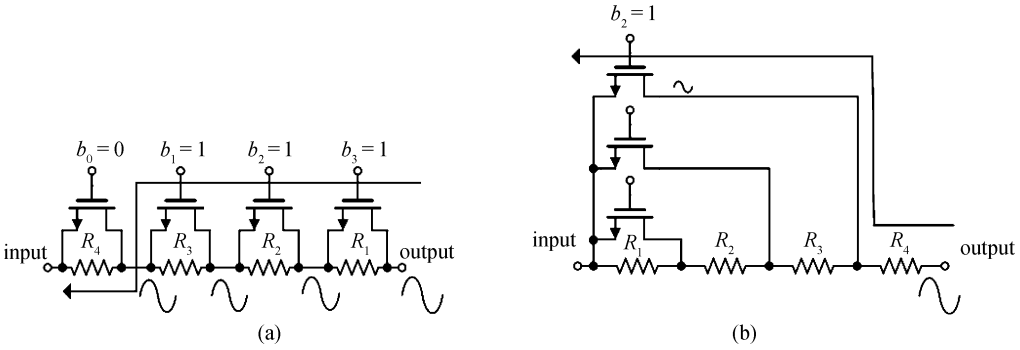

Fig. 4. (a) Variable resistor. (b) High linearity variable resistor.

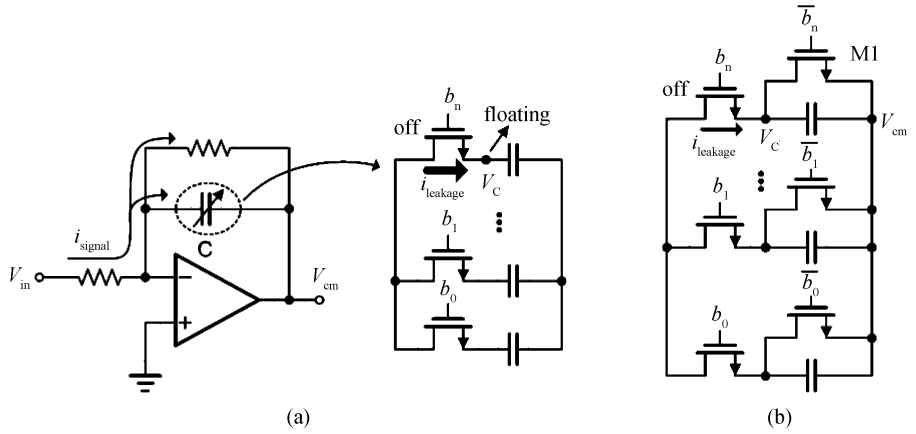

Fig. 5. (a) First-order filter with switchable capacitor. (b) Switchable capacitor array with the proposed CB technique.

With the scaling down of the power supply, the linearity performance of analog circuits is becoming challenging. The main baseband filter's nonlinearity contributors are the nonlinearity of operational amplifiers, the on-state switches used in resistor arrays and the subthreshold leakage current of the off-state switches used in capacitor arrays. The nonlinearity contribution of the operational amplifier can be reduced by using miller OTA for high output swing and increasing the operational amplifier's GBW[4]. To facilitate digital gain control, the variable resistors are realized by the linear resistors in series with the MOSFET switches biased in the triode region. The switched resistor arrays shown in Figs. 4(a) and 4(b) have different linearity performances. As shown in Fig. 4(a), the large output signal passes through the on switches and induced high distortion, because the resistor value of the switches is dependent on source voltage. As shown in Fig. 4(b), the MOSFET switches are usually connected to the virtual ground, such as the summing node of the feedback network. The large output signal passes the linear resistor before on-switches and the voltage swing of the MOSFET source is smaller. The linearity performance is greatly enhanced.

Due to the high leakage current in deep-submicrometer process, the linearity of the filter with switched capacitor array is deteriorated. The leakage current can be expressed as[5]

$$I_{ds}=\frac{W_{eff}}{L_{eff}}\mu\sqrt{\frac{q\varepsilon_{si}N_{cheff}}{2\Phi_s}}v_T^2 e^{\frac{V_{gs}-V_{th}}{nv_T}}\left(1-e^{\frac{-V_{ds}}{v_T}}\right), \quad (6)$$

where N_{cheff} is the effective channel doping, Φ_s is the surface potential, n is the subthreshold swing, and v_T is the thermal voltage given by kT/q. The leakage current reduces substantially with decreasing the source potential (V_s). Figure 5(a) shows a first order low pass filter with switched capacitor array. The switched off capacitors after tuning and cut-off frequency switching process make the NMOS source floating. The voltage of the floating point is determined by the drain-to-source leakage, source-to-substrate leakage and source-to-gate leakage. The voltage of the floating point is normally far lower than the output common mode voltage of the operational amplifier and the floating point has the same voltage swing as the operational amplifier's output. Due to the exponential relation between the leakage current and the negative source voltage ($-V_s$) in Eq. (6), the large source voltage swing with lower common mode potential leads to a larger leakage current. As shown in Fig. 5(a), the nonlinear leakage current directly contributes to the signal. Figure 5(b) shows the switchable capacitor array with the proposed CB technique. The source of NMOS switch is no longer floating but connected to the output through switched-on bypass transistor (M1). So the voltage at the source of the switch is higher than when it is floating and the nonlinear leakage current is reduced. The simulation result shows that the in-band IIP3 is improved from 32 to 47 dBm.

4. Operational amplifier design

The required specification of the operational amplifier used in active-RC filter can be defined from the active-RC integrator, and the GBW requirement can expressed as[6]

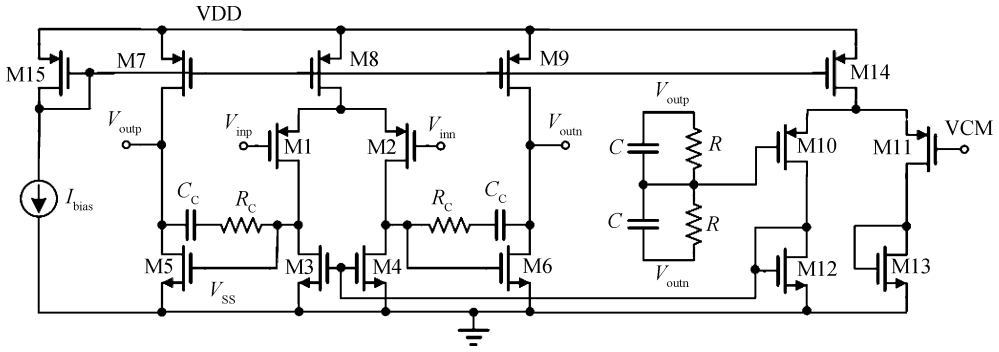

Fig. 6. Schematic of the operational amplifier.

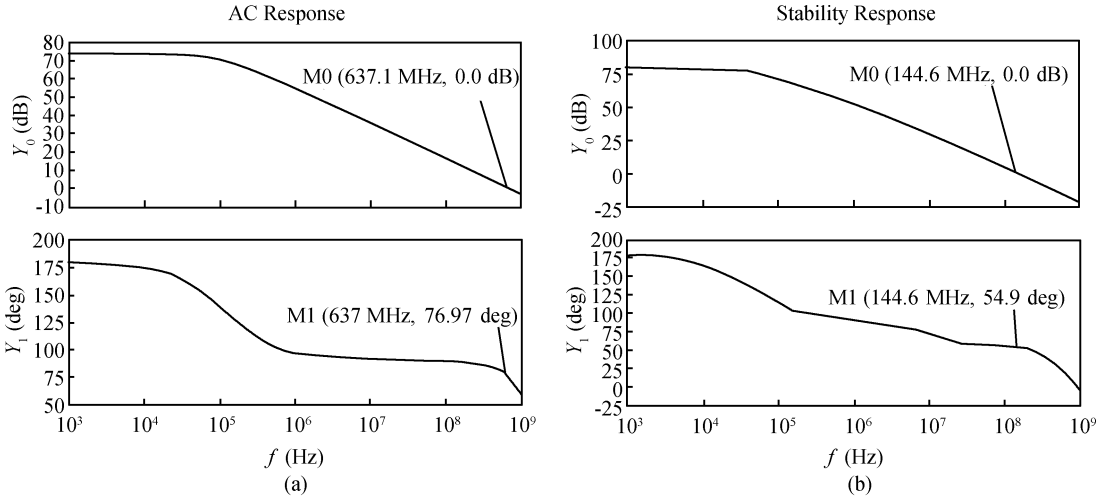

Fig. 7. (a) Differential-mode opamp bode plot. (b) Common-mode opamp bode plot.

$$\mathrm{GBW} \geqslant \left|\frac{A_{\mathrm{C}}(j\omega_{\mathrm{C}})}{\delta} - 1\right| \left|[1 + A_{\mathrm{C}}(j\omega_{\mathrm{C}})]\omega_{\mathrm{C}}\right|, \tag{7}$$

where $A_{\mathrm{c}}(j\omega_{\mathrm{C}})$ is defined as close loop gain, ω_{C} is the cut-off frequency of the filter, and δ is the error between the real transfer function and the ideal transfer function. A miller OTA shown in Fig. 6 is adopted for its high output swing. Figures 7(a) and 7(b) show the simulation results of the operational amplifier. The differential GBW is 637 MHz with 76° phase margin and the common-mode GBW is 144 MHz with 54° phase margin.

As mentioned above, the noise of the last operational amplifier should be limited. Because the out-of-band noise is mainly contributed by the thermal noise, the equivalent input noise voltage can be expressed as

$$\begin{aligned}\overline{\mathrm{d}v_{\mathrm{ieq}}^2} &\approx \frac{2\,(4kT\gamma g_{\mathrm{m1}} + 4kT\gamma g_{\mathrm{m3}})}{g_{\mathrm{m1}}^2}\mathrm{d}f \\ &= \frac{1}{g_{\mathrm{m1}}}\left(8kT\gamma + \frac{8kT\gamma g_{\mathrm{m3}}}{g_{\mathrm{m1}}}\right),\end{aligned} \tag{8}$$

where g_{m1} and g_{m3} are the transconductances of M1 and M3 respectively. From Eq. (8), the equivalent input noise can be reduced by increasing g_{m1}. A large g_{m1} can be achieved by increasing power consumption and reducing $V_{\mathrm{GS}} - V_{\mathrm{T}}$ for the two input transistors.

5. Automatic tuning circuit design

The AFT is necessary for active-RC filter due to the process spread of ±20% for R and C which affects the cut-off frequency directly and causes the deterioration of EVM. The capacitor-based frequency tuning is favored over resistor-based frequency tuning method[7]. An on-chip auto-calibration by comparing its RC time constant with a reference clock is shown in Fig. 8. The current of including the process variation of R can be expressed as $I_1 = V_{\mathrm{ref}}/R$, and the capacitor voltage, V_{cap} is discharged by $\mathrm{S_0}$. When $\mathrm{S_1}$ is closed, the capacitor C is charged for the time interval Δt and the charge current I_2 mirrored I_1. After the charge, $\mathrm{S_1}$ is opened and $\mathrm{S_2}$ is closed, the comparator compares V_{cap} with V_{ref}, the compared result V_{cmp} controls the digital algorithm to tuning the capacitor array. When $V_{\mathrm{cap}} = V_{\mathrm{ref}}$, the tuning process is finished. The tuning process can be expressed as

$$V_{\mathrm{cap}} = \frac{Q}{C} = \frac{I_2\Delta t}{C} = \frac{I_1\Delta t}{C} = \frac{V_{\mathrm{ref}}}{RC}\Delta t, \tag{9}$$

to make $V_{\mathrm{cap}} = V_{\mathrm{ref}}$,

$$RC = \Delta t, \tag{10}$$

where Δt is the reference clock period. This means that R and C products is free from process variation and the cut-off frequency is tuned precisely. A 9-bit capacitor array is used for

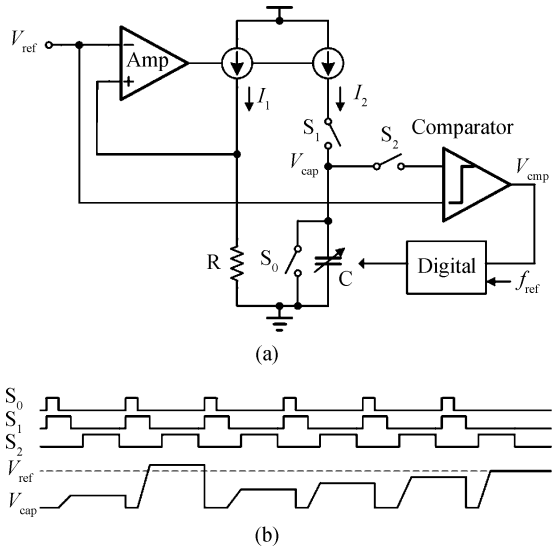

Fig. 8. (a) Automatic frequency tuning circuit. (b) Timing diagram.

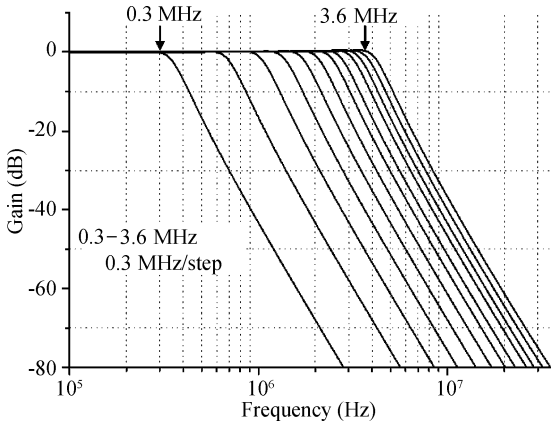

Fig. 9. Frequency response of baseband filter.

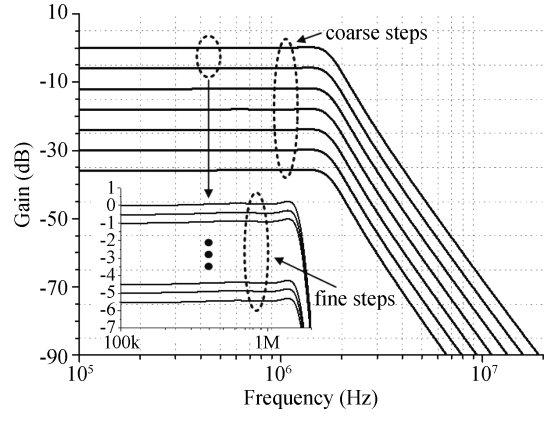

Fig. 10. Gain settings for baseband filter.

AFT and cut-off frequency switching. To ensure the tuning error under ±5%, 6-bit is adopted for tuning and the cut-off frequency switching process is done after tuning process.

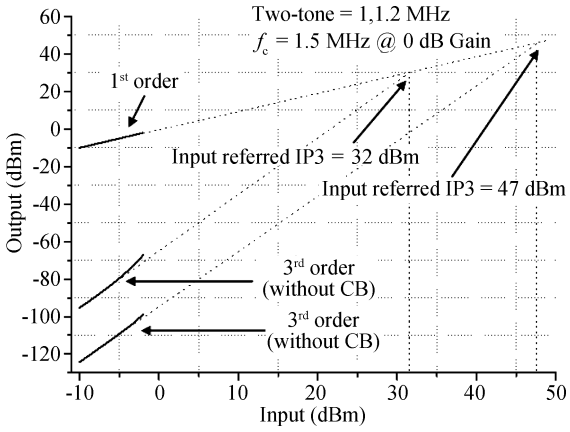

Fig. 11. Baseband filter linearity performance.

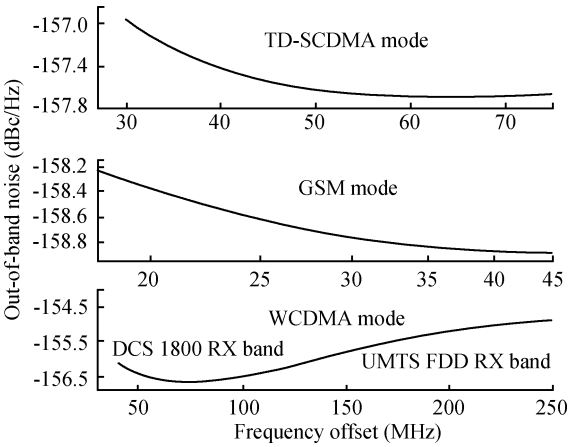

Fig. 12. TD-SCDMA , GSM and WCDMA out-of-band noise.

Table 1. Summary of the baseband filter.

Parameter	Value
Technology	0.13 μm CMOS process
Supply voltage	1.2 V
Power consumption	3.6 mA × 1.2 V = 4.32 mW
Cut-off frequency	0.3–3.6 MHz, 0.3 MHz/step
Gain range	–40 to 0 dB, 0.5 dB/step
In-band IIP3	47 dBm
Out-of-band noise	–156 dBc/Hz @ WCDMA
	–157 dBc/Hz @ TD-SCDMA
	–158 dBc/Hz @ GSM

6. Simulation results

A 4th order low pass baseband filter with AFT is designed in 0.13 μm CMOS technology. The filter frequency response is shown in Fig. 9. The cut-off frequency can be switched from 0.3 to 3.6 MHz in 0.3 MHz steps. Figure 10 shows the gain settings, the gain range is –40 to 0 dB in 0.5 dB steps. Figure 11 shows the in-band IIP3 at 1.5 MHz cut-off frequency and 0 dB gain. By using the proposed CB technique, the filter achieves 47 dBm in-band IIP3 which is 15 dB better than the one without CB technique. The simulated out-of-band noise in Fig. 12 shows that the baseband filter can meet the requirement of SAW-less WCDMA and TD-SCDMA transmitter. The SAW-less GSM transmitter under 1.2-V power supply is diffi-

Table 2. Performance comparison.

Reference	Ref. [8]	Ref. [9]	Ref. [10]	This work (simulation results)
Topology	Active-RC	Active-RC	Active-RC	Active-RC
Supply voltage (V)	1.5	1	1.2	1.2
Filter order	5	1/3/5	3/5	4
Power (mW)	11.25	3.0–7.5	4.6	4.32
Bandwidth (MHz)	19.7	1–20	5, 10	0.3–3.6
In-band IIP3 (dBm)	18.3	31.3	20	47

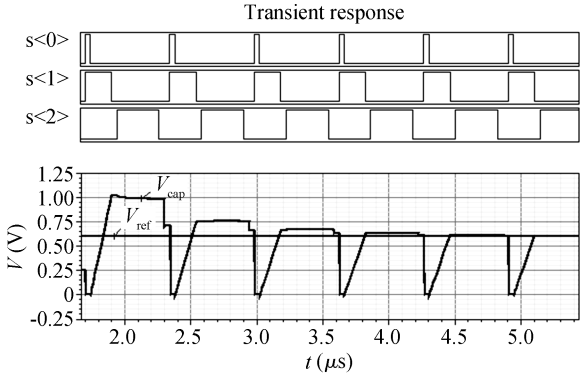

Fig. 13. Automatic frequency tuning.

cult to implement. By using smaller R and reducing the equivalent input noise voltage of the last operational amplifier shown in Fig. 1, the out-of-band noise can meet the requirement of SAW-less GSM transmitter. But the filter's power consumption will become unaffordable. Another method to achieve SAW-less GSM transmitter is to improve the power supply. A higher power supply can achieve higher signal to noise ratio and meet the requirement of SAW-less GSM transmitter. The out-of-band noise of LPF can also be filtered in modulator but with the penalty of area and power consumption. The result in Fig. 13 shows the cut-off frequency can be tuned to the right setting. The performance of the baseband filter is summarized in Table 1, and a performance comparison is given in Table 2.

7. Conclusion

A 4th order reconfigurable low pass baseband filter for GSM, TD-SCDMA and WCDMA multi-mode transmitter is presented. A capacitor bypass technique is proposed to improve the filter's linearity performance. The out-of-band noise meets TD-SCDMA and WCDMA applications. The baseband filter can provide 40 dB gain control range for the transmitter. The cut-off frequency can be reconfigured flexibly for the multi-mode transmitter applications. To reduce the out-of-band noise, the last operational amplifier shown in Fig. 1 consumes more than half of the filter's power consumption.

References

[1] UE radio transmission and reception (FDD) technical specifications 25.101,V8.5.1. 3rd Generation Partnership Project (3GPP), 2009

[2] He X, van Sinderen J. A low-power, low-EVM, SAW-less WCDMA transmitter using direct quadrature voltage modulation. IEEE J Solid-State Circuits, 2009, 44(12): 3448

[3] Gu Q. RF system design of transceivers for wireless communications. New York: Springer, 2005

[4] Gray P R, Meyer R G. Analysis and design of analog integrated circuits. 3rd ed. New York: John Wiley & Sons, 1993

[5] Mukhopadhyay S, Raychowdhury A, Roy K. Accurate estimation of total leakage in nanometer-scale bulk CMOS circuit based on device geometry and doping profile. IEEE Trans Computer-Aided Design of Integrated Circuits and System, 2005, 24(3): 363

[6] Du D, Li Y, Wang Z. An active-RC complex filter with mixed signal tuning system for low-IF receiver. IEEE Asia Pacific Conference on Circuits and Systems, 2006: 1031

[7] Khalil W, Chang T Y, Jiang X, et al. A Highly integrated analog front-end for 3G. IEEE J Solid-State Circuits, 2003, 38(5): 774

[8] Kousai S, Hamada M, Ito R, et al. A 19.7 MHz, fifth-order active-RC Chebyshev LPF fo draft IEEE802.11n with automatic quality-factor tuning scheme. IEEE J Solid-State Circuits, 2007, 42(11): 2326

[9] Amir-Aslanzadeh H, Pankratz E, Sanchez-Sinencio E. A 1-V +31 dBm IIP3, reconfigurable, continuously tunable, power-adjustable active-RC LPF. IEEE J Solid-State Circuits, 2009, 44(2): 495

[10] Vasilopoulos A, Vitzilaios G, Theodoratos G, et al. A low-power wideband reconfigurable, integrated active-RC filter with 73 dB SFDR. IEEE J Solid-State Circuits, 2006, 41(9): 1997